NRF2 activation in BON-1 neuroendocrine cancer cells reduces the cytotoxic effects of a novel Ruthenium(II)-curcumin compound: A pilot study

ALESSIA GARUFI[1], RICCARDO PETTINARI[2], LAURA MONTEONOFRIO[1], GIULIA PULIANI[3], ILARIA VIRDIA[1], MARIALUISA APPETECCHIA[3], FABIO MARCHETTI[4], MARA CIRONE[5], SILVIA SODDU[1] and GABRIELLA D'ORAZI[1,6,7]

[1]Unit of Cellular Networks and Molecular Therapeutic Targets, IRCCS Regina Elena National Cancer Institute, I-00144 Rome; [2]Chemistry Interdisciplinary Project (CHIP), School of Pharmacy, University of Camerino, I-62032 Camerino (MC); [3]Oncological Endocrinology Unit, IRCCS Regina Elena National Cancer Institute, I-00144 Rome; [4]Chemistry Interdisciplinary Project (CHIP), School of Science and Technology, University of Camerino, I-62032 Camerino (MC); [5]Department of Experimental Medicine, Sapienza University of Rome, Laboratory Affiliated to Pasteur Institute Italy Foundation Cenci Bolognetti, I-00161 Rome; [6]UniCamillus International University of Health Sciences, School of Medicine, I-00100 Rome; [7]Department of Neurosciences, Imaging and Clinical Sciences, University 'G. D'Annunzio', I-66013 Chieti, Italy

Received July 31, 2023; Accepted December 18, 2023

DOI: 10.3892/or.2024.8695

Abstract. Gastroenteropancreatic neuroendocrine neoplasms (GEP-NEN) are a group of rare tumors whose specific pathogenetic mechanisms of resistance to therapies have not been completely revealed yet. Chemotherapy is the main therapeutic approach in patients with GEP-NEN, however, novel combination regimens and targeted therapy are continuously explored. In the present study, the anticancer effect of a novel Ruthenium (Ru)(II)-Bisdemethoxycurcumin (Ru-bdcurc) compound was evaluated in BON-1 cell line, one of the few cell lines derived from GEP-NEN, largely used in experimental research of this type of tumors. The experimental data revealed that the Ru-bdcurc compound induced cell death in a dose-dependent manner, *in vitro*. Biochemical studies demonstrated that, in response to the lower dose of treatment, BON-1 cells activated the nuclear factor erythroid 2-related factor 2 (NRF2) pathway with induction of some of its targets including catalase and p62 as well as of the antiapoptotic marker Bcl2, all acting as chemoresistance mechanisms. NRF2 induction associated also with increased expression of endogenous p53 which is reported to be dysfunctional in BON-1 cells and to inhibit apoptosis. Genetic or pharmacologic targeting of NRF2 inhibited the activation of the NRF2 pathway, as well as of endogenous dysfunctional p53, in response to the lower dose of Ru-bdcurc, increasing the cell death. To assess the interplay between NRF2 and dysfunctional p53, genetic targeting of p53 showed reduced activation of the NRF2 pathway in response to the lower dose of Ru-bdcurc, increasing the cell death. These findings identified for the first time a possible dysfunctional p53/NRF2 interplay in BON-1 cell line that can be a novel key determinant in cell resistance to cytotoxic agents to be evaluated also in GEP-NEN.

Correspondence to: Professor Gabriella D'Orazi, Department of Neurosciences, Imaging and Clinical Sciences, University 'G. D'Annunzio', 31 Via dei Vestini, I-66013 Chieti, Italy
E-mail: gdorazi@unich.it

Dr Alessia Garufi, Unit of Cellular Networks and Molecular Therapeutic Targets, IRCCS Regina Elena National Cancer Institute, 53 Via Elio Chianesi, I-00144 Rome, Italy
E-mail: alessia.garufi@ifo.it

Key words: gastroenteropancreatic neuroendocrine tumors, BON-1 cells, nuclear factor erythroid 2-related factor 2, p53, chemoresistance, ruthenium-curcumin compounds, apoptosis, brusatol

Introduction

Gastroenteropancreatic neuroendocrine neoplasms (GEP-NENs) are a group of rare tumors originating from neuroendocrine cells of the pancreas or of the gastrointestinal tract and comprise well-differentiated neuroendocrine tumors (NETs) and poorly-differentiated neuroendocrine carcinomas (NECs) (1). Moreover, depending on the hormone and amine secretion activity, GEP-NENs can be classified into functional and non-functional neoplasms (2). They represent the second most common cancer of the digestive system as their incidence has increased over the last decades (3). GEP-NENs are characterized by an indolent behavior in terms of tumor growth and the treatment of choice in locally defined tumors remains surgical resection (4). However, at presentation, ~80% of patients have already developed liver or lymph node metastases (5). The number of targeted and theranostic options for patients with NETs have expanded significantly over the

last decade; however, the cytoreductive capacity of these agents remains quite modest (6). Thus far, chemotherapy has demonstrated to be clinically useful in patients with metastatic or unresectable pancreatic NETs and grade 3 NET disease, however, novel combination regimens and targeted therapy are necessary to increase the number of cytotoxic options that may be relevant for patients with NETs (6,7).

Numerous anticancer studies have focused lately on natural compounds, present in fruits, vegetables and spices, that exhibit pro-apoptotic and anti-inflammatory activity by targeting diverse molecules including transcription factors, cytokines, chemokines, growth factor receptors and inflammatory enzymes (8). In addition, for their easy availability, safety and relative low-cost, natural compounds are particularly attractive for chemoprevention (8). Among the natural compounds, curcumin, a hydrophobic polyphenol has been revealed to possess anticancer properties along with an excellent safety profile although it presents low solubility and bioavailability (9,10). To circumvent this latter problem, a number of strategies have been developed, involving the modification of its structure or application of drug delivery agents, such as nanoparticles, liposomes and micelles (11). Another approach is based on the interaction of curcumin ligands with inorganic or organometallic ruthenium moieties to provide more soluble and assimilable compounds (12-14) that are more attractive for clinical practice. Those compounds are stable and water-soluble and their frameworks provide considerable scope for optimizing the design in terms of their biological activity and for minimizing side-effects. For these reasons, organometallic ruthenium compounds are promising anticancer molecules to be tested in clinical practice especially in combination with other drugs (15-17). It was recently demonstrated by the authors the anticancer effects of ruthenium(II)-curcumin compounds *in vitro* in different cancer cell lines including colon, breast and glioblastoma (18,19), as well as their lack of toxicity in normal cells (16). However, to the best of the authors' knowledge, these compounds have never been used in neuroendocrine tumors.

Different from normal cells, cancer cells often activate an adaptive response to resist to the anticancer treatments (20). In this regard, the authors' recent studies demonstrated the role of the nuclear factor erythroid 2-related factor 2 (NRF2)-induced pathway as key determinant in cancer cells' resistance to therapies (18,19,21). NRF2 transcription factor is the master regulator of the oxidative stress and its detoxifying activity is often hijacked by cancer cells as a protective mechanism, particularly in the course of anti-cancer treatments, leading to cancer cell resistance to therapies (22). Among the NRF2 targets, involved in cancer progression and chemoresistance, is heme-oxygenase 1 (HO-1), catalase, NAD(P)H quinone oxidoreductase 1 (NQO1) and p62/SQSTM (herein p62) (22,23). Intriguingly, NRF2 induces p62 expression and p62 stabilizes NRF2 by triggering the degradation of NRF2 inhibitor Kelch-like ECH-associated protein 1 (Keap1), creating a positive feedback loop between NRF2 and p62 that induces cancer progression and resistance to therapies (24,25). NRF2 is often overexpressed in pancreatic cancer which may reflect a greater intrinsic capacity of the tumor cells to respond to stress signals and resist to the chemotherapeutic agents (26). However, to the best of the authors' knowledge, NRF2 activity has never been evaluated in the pancreatic NET cell line BON-1, one of the two commonly used human cell line GEP-NET-derived, which also carries an endogenous dysfunctional p53 that inhibits apoptosis (27-29). Among the oncogenic pathways that establish a cross-talk with NRF2, other than p62, is mutant (mut) p53 (30). Tumor suppressor p53 plays a central role in tumor prevention and in response to anticancer therapies and, for these reasons, is the most inactivated oncosuppressor in human tumors, by gene mutation or by protein deregulation (31,32). TP53 gene mutations have been found in pancreatic cancer affecting both cancer progression and response to therapies (33), and also in poorly differentiated NEC (34). In BON-1 cell line, a homozygous stop-gain g.7574003A>G mutation has been found in exon 10 of TP53 with possible inhibition of the p53 apoptotic activity (28).

On the basis of the aforementioned background, in the present study it was aimed to evaluate the anticancer effects of the cationic Ruthenium (Ru)(II)-Bisdemethoxycurcumin compound (Ru-bdcurc) in the cell line BON-1. The present study highlighted the key role of NRF2 in BON-1 resistance to the cytotoxic activity of the curcumin compound and the interplay of NRF2 with a dysfunctional endogenous p53, supporting the monitoring of this potential biomarker in neuroendocrine tumors for future assessment of response to therapies.

Materials and methods

Cell culture and reagents. In the present study, the BON-1 cell line (RRUD: CVCL_3985) (NCL2110P096; DBA Italia s.r.l.) (https: www.cellosaurus.org/CVCL_3985), established from a lymph node metastasis of a human pancreatic carcinoid tumor (27), was used. Cells arrived at passage 1 and were used for additional 6 passages. Cells were maintained in Dulbecco's modified Eagle's medium (DMEM) (Invitrogen; Thermo Fisher Scientific, Inc.) supplemented with 10% heat-inactivated fetal bovine serum (FBS) (Corning, Inc.), plus glutamine and antibiotics [Penicillin-Streptomycin-L-Glutamine, 100x (+) 29.2 mg/ml L-glutamine; cat. no. 30-009-CI; Merck KGaA] in a humidified atmosphere with 5% CO_2 at 37˚C. Cells underwent routine testing to ensure that they were mycoplasm negative. The cationic Ruthenium (Ru)(II) compound containing bisdemethoxycurcumin and the hydrosoluble PTA phosphine ([(cym)Ru(bdcurc)(PTA)]SO3CF3) (where cym=cymene, bdcurc=bisdemethoxycurcumin and PTA=1,3,5-triaza-7-phosphaadamantane) (herein Ru-bdcurc), with the chemical formula: C36H42F3N3O7PRuS and the molecular weight: 849,8 g/mol, was synthesized as previously reported (16,17). The Ru-bdcurc compound was dissolved in DMSO and stored at -20˚C before using it at 50 and 100 μM for the indicated times, as previously reported (19). The inhibitor of the antioxidant response Brusatol (cat. no. SML1868; Sigma-Aldrich; Merck KGaA) (35,36) was used at 100 μM for 4 h pre-treatment, as previously reported (37).

Cell viability and colony assays. Cell viability was measured by Trypan blue (cat. no. 72571; Sigma-Aldrich; Merck KGaA) assay. Subconfluent cells were plated in six-well plates and, the day after, treated with different concentration of Ru-bdcurc

for 24 and 48 h or in combinations with a 4 h pre-treatment of NRF2 inhibitor Brusatol (100 nM). After treatments, both floating and adherent cells were collected and stained with Trypan blue. Cell viability of triplicates was assessed by counting blue (dead)/total cells with a Neubauer hemocytometer using light microscopy. For long-term cell survival, cells were plated in 60 mm Petri dishes until subconfluence. Then, cells were mock-treated or treated with Ru-bdcurc (50 or 100 μM) for 16 h. After treatments, cells were washed, trypsinized, counted and equal cell number re-plated in duplicate with fresh medium in 60-mm Petri dishes for determining cell survival. Death-resistant colonies (with >50 cells) were stained with crystal violet (cat. no. 46364; Sigma-Aldrich; Merck KGaA) (diluted 1:2 with the cell culture) 14 days later. Plates underwent scanning and the intensity of the cell staining was quantified by ImageJ software.

Western blot analysis. Cells were harvested and centrifuged and the resulting pellets were lysed in lysis buffer (50 mM Tris-HCl, pH 7.5, 150 mM NaCl, 5 mM EDTA, 150 mM KCl, 1 mM dithiothreitol and 1% Nonidet P-40) (all from Sigma-Aldrich; Merck KGaA) containing protease inhibitors (CompleteTM, Mini Protease Inhibitor Cocktail; Merck Life Science S.r.l.). Protein concentration was determined by the Bio-Rad protein assay kit (cat. no. 5000001; Bio-Rad Laboratories, Inc.), a simple colorimetric assay for measuring total protein concentration based on the Bradford dye-binding method. Proteins were separated by loading 10-30 μg of total cell lysates on denaturing 8-15% SDS-PAGE (polyacrylamide gel electrophoresis) gels (Bio-Rad Laboratories, Inc.), following semidry blotting to polyvinylidene difluoride (PVDF) membranes (Immobilon-P; Merck KGaA). Unspecific signals were blocked by incubating the membranes in Tris-buffered saline containing 0.1% Tween 20 (TBS) and 3% BSA (Sigma-Aldrich; Merck KGaA) for 1 h at room temperature. Membranes were then probed with the primary antibodies and subsequently with the following secondary antibodies: Goat Anti-Mouse IgG (1:10,000; cat. no. 1706516) and Goat Anti-Rabbit IgG (1:10,000; cat. no. 1706515; both from Bio-Rad Laboratories, Inc.). The enzymatic signal was visualized by chemiluminescence (ECL Detection system; Amersham; Cytiva). The following antibodies were used: Mouse monoclonal anti-p62/SQSTM1 (D-3; 1:1,000; cat. no. sc-28359), mouse monoclonal anti-catalase (H-9; 1:1,000; cat. no. sc-271803), mouse monoclonal anti-p53 (DO-1; 1:1,000; cat. no. sc-126), mouse monoclonal anti-Bcl-2 (1:1,000; cat. no. sc-509) and mouse monoclonal anti-Mcl1 (G-7; 1:1,000; cat. no. sc-74437) (all from Santa Cruz Biotechnology, Inc.), rabbit polyclonal anti-NRF2 (1:1,000; cat. no. ab62352; Abcam), mouse monoclonal anti-phospho-Histone H2AX (Ser139 clone JBW301; 1:1,000; cat. no. 05-636; Sigma-Aldrich; Merck KGaA), rabbit polyclonal anti-phospho-4E-BP1 (Thr37/46; 1:200; ca.t no. 2855), rabbit polyclonal anti-4E-BP1 (1:200; cat. no. 9452; both from Cell Signaling Technology, Inc.), mouse monoclonal anti-poly(ADP-ribose) polymerase (PARP, cleavage site-214-215; 1:1,000; cat. no. AB3565; Sigma-Aldrich; Merck KGaA). Mouse monoclonal β-actin (Ab-1; 1:10,000; (cat. no. CP01; Calbiochem; Merck KGaA), was used as protein loading control.

Densitometric analysis. Densitometry was performed on ECL results with ImageJ software (1.47 version; National Institutes of Health) which was downloaded from the NIH website (http://imagej, nih.gov/ij) and the relative band intensity was normalized to β-actin signals and plotted as protein expression/β-actin ratio.

Small interference (si)RNA transfection. Cells were plated at subconfluency in 35-mm Petri dishes and, the day after plating, were transfected with the Nrf2 small interference (si)RNA (cat. no. sc-37030) or control siRNA (cat. no. sc-37007) (both from Santa Cruz Biotechnology, Inc.; the siRNA sequences are not available) using LipofectaminePLus reagent (cat. no. 11514015; Thermo Fisher Scientific, Inc.) as previously reported (18). The concentration used was 10 nmol. For p53 knockdown, cells were transfected with sip53 plasmid (sip53) or an empty vector (si-ctr) (38,39) using LipofectaminePLus reagent according to the manufacturer's instructions. A total of 24 h after transfection, cells were trypsinized and replated for the indicated experiments.

RNA extraction and semiquantitative reverse transcription (RT)-polymerase chain reaction (PCR) analysis. Total RNA extraction was performed by using TRIzol Reagent (Thermo Fisher Scientific, Inc.), according to the manufacturer's instructions. cDNA was synthesized by using MuLV reverse transcriptase kit according to the manufacturer's instructions (Applied Biosystems; Thermo Fisher Scientific, Inc.). Semiquantitative RT-PCR was carried out with 2 μl cDNA reaction and genes specific oligonucleotides under conditions of linear amplification. by using Hot-Master Taq polymerase (Thermo Fisher Scientific, Inc.). Primer sequences specific to the target genes were as follows: HO-1 forward, 5'AAGATT GCCCAGAAAGCCCTGGAC-3' and reverse, 5'-AACTGT CGCCACCAGAAAGCTGAG-3' (40) (annealing temperature: 58˚C for 30 cycles); p62 forward, 5'-CTGCCCAGACTA CGACTTGTGT-3' and reverse, 5'-TCAACTTCAATGCCCA GAGG-3' (19,40) (annealing temperature: 58˚C for 28 cycles); NRF2 forward, 5'-TCCATTCCTGAGTTACAGTGTCT-3' and reverse, 5'-TGGCTTCTGGACTTGGAACC-3' (18,40,41) (annealing temperature: 58˚C for 30 cycles); MDR1 forward, 5'-AACGGAAGCCAGAACATTCC-3' and reverse, 5'-AGG CTTCCTGTGGCAAAGAG-3' (42,43) (annealing temperature: 60˚C for 29 cycles); 28S forward, 5'-GTTCACCCACTA ATAGGGAACGTGA-3' and reverse, 5'-GGATTCTGACTT AGAGGCGTTCAGT-3' (39,40,44,45) (annealing temperature: 58˚C for 15 cycles) ; Bcl-2 forward, 5'-AGGATTGTG GCCTTCTTTGAG-3' and reverse, 5'-GAGACAGCCAGG AGAAATCAAA-3' (46) (annealing temperature: 58˚C for 30 cycles); and NOXA forward, 5'-AGGACTGTTCGTGTT CAGCTC-3' and reverse 5'-GTCCACCTCCTGAGAAAA CTC-3' (47) (annealing temperature: 55˚C for 28 cycles). The denaturation and extension temperatures were, respectively 98 and 72˚C for all the mRNA amplifications. PCR products were run on a 2% agarose gel and visualized with GelRed Nucleic Acid gel stain (Biotium, Inc.). The housekeeping 28S gene, used as internal standard, was amplified from the same cDNA reaction mixture. Densitometric analysis was applied to quantify mRNA levels compared with 28S control gene expression.

Statistical analysis. The results are expressed as the mean ± standard deviation (SD) of at least three independent experiments and statistical analyses were performed using GraphPad Prism® software (Version 9.0.0; Dotmatics). The unpaired two-tailed Student t-test (for data containing two groups) and the nonparametric 1-way analysis of variance (ANOVA) followed by Tukey's HSD test (for multiple comparisons tests) were used to demonstrate statistical significance. A difference was considered statistically significant when $P \leq 0.05$.

Results

Ru-bdcurc compound induces dose- and time-dependent BON-1 cells' death. BON-1 cells were treated with two concentrations of Ru-bdcurc compound that were recently demonstrated by the authors to have different cytotoxic activity against colon cancer cells (19). The results revealed a dose- and time-dependent cell death, as indicated by the trypan blue assay (Fig. 1A). Cell death was also evidenced microscopically where distinct signs of cell shrinkage were observed, in particular at 100 μM dose of Ru-bdcurc (Fig. 1B). The EC50 for the Ru-bdcurc compound was 100 μM (AAT Bioquest, Inc; https://www.aatbio.com/tools/ic50-calculator). Then the long-term survival was analyzed by colony formation assay. The results of the densitometric analysis demonstrated that 100 μM dose of Ru-bdcurc significantly reduced BON-1 cell survival, compared with 50 μM dose (Fig. 1C). At the biochemical level, the occurrence of an apoptotic cell death, as indicated by the cleaved fragment of PARP (clPARP) and by the increased clPARP/PARP ratio, was evident only with the 100 μM dose treatment, compared with 50 μM dose (Fig. 1D). The apoptotic cell death associated with the appearance of the phosphorylated form of H2AX (γH2AX) (Fig. 1D), a marker of DNA damage and apoptosis (48). Then the phosphorylation of 4EBP1 (p4E-BP1), a mTOR target whose activation can sustain cancer cell survival and predict poor prognosis (49,50), was investigated. In agreement, mTOR pathway has been found dysregulated in GEP-NET and involved in tumor development (51). As shown in Fig. 1D, p4E-BP1 was induced by 50 μM dose, on the other hand, p4E-BP1 was impaired by 100 μM dose of Ru-bdcurc. This latter result associated with the greater induction of cell death that was observed by using 100 μM dose of Ru-bdcurc, compared with 50 μM dose, strengthening the antiapoptotic role of p4E-BP1. Collectively, these results indicated that 100 μM dose of Ru-bdcurc induced BON-1 cell death while 50 μM dose activated survival pathways that potentially reduced the compound cytotoxic effects.

NRF2 pathway activation in response to 50 μM dose of Ru-bdcurc. Several lines of evidence suggest the important role of NRF2 in the chemoresistance of different types of cancer cells (22), as also assessed by the authors' recent studies using curcumin compounds (18,19). However, to the best of the authors' knowledge, NRF2 has never been evaluated in BON-1 cells. Therefore, the NRF2 pathway in BON-1 cells in response to the Ru-bdcurc treatment was next assessed. To this aim, the two doses of the compound, that were revealed to have different outcome in terms of cell death as aforementioned, were used. The experimental data demonstrated that 50 μM dose of Ru-bdcurc significantly increased the levels of NRF2 protein, compared with the 100 μM dose, and induced the expression of its targets such as catalase and p62 (Fig. 2A). To evaluate if the NRF2 induction was at the transcriptional or post-transcriptional level, mRNA analysis was performed. It was identified that 50 μM dose of Ru-bdcurc did not induce NRF2 gene expression (Fig. 2B), suggesting rather stabilization of NRF2 at the protein level. In addition, only the 50 μM dose increased the mRNA expression of the NRF2 targets HO-1 and p62 (Fig. 2B), indicative of NRF2 transcriptional activation, in this setting. Thus, the increased p62 gene expression was in accordance with the finding that p62 is a NRF2 transcriptional target (23-25). Interestingly, it has been reported that p62 activates pro-survival pathways including mTOR (52), in agreement with the aforementioned results in Fig. 1 and with the cross-talk among oncogenic pathways such as p62/mTOR/NRF2 to increase tumor development and resistance to therapies (30). In agreement with the different extent of cell death in response to different doses of Ru-bdcurc, the results showed that only 50 μM dose of Ru-bdcurc increased the antiapoptotic Bcl-2 protein levels while the 100 μM dose significantly reduced the levels of Mcl1 protein (Fig. 2A), a pro-survival member of the Bcl-2 family (53). Moreover, 50 μM dose of Ru-bdcurc treatment, compared with 100 μM dose, increased the endogenous p53 protein level (Fig. 2A), in agreement with the paradigm of NRF2/mutp53 interplay to sustain their oncogenic activities (41,54). The endogenous p53 is reported to be dysfunctional in BON-1 cells and inhibit apoptosis (28). In agreement, the present results revealed that 50 μM dose of Ru-bdcurc, compared with 100 μM dose, induced the expression of multidrug resistant gene 1 (MDR1), a target of some mutant p53 proteins (55), as well as of the antiapoptotic gene Bcl-2 (Fig. 2B), which associated with a potential oncogenic activity of the endogenous dysfunctional p53 in BON-1 cells. On the other hand, 100 μM dose of Ru-bdcurc induced the expression of Noxa (Fig. 2B), a pro-apoptotic gene induced by p53 family members (56), that has been shown to inhibit the antiapoptotic Mcl1 protein (57). This latter result is in consistency with the reduction of Mcl1 protein levels in Fig. 2A and with induction of the apoptotic cell death (Fig. 1A). Taken together, these findings indicated that the Ru-bdcurc treatment was able to induce pro-apoptotic (PARP cleavage, Fig. 1) or cell death-resistant pathways (NRF2-induced targets, mTOR target 4E-BP1, Bcl-2 and dysfunctional p53; Fig. 2) according to the low (50 μM) or high (100 μM) dose used.

Targeting NRF2 improves the cytotoxic activity of 50 μM dose of Ru-bdcurc. Then, to evaluate the biological role of NRF2 in this setting, it was attempted to inhibit it by pharmacologic or genetic means. NRF2 pharmacologic inhibitor Brusatol (35,36) was used before exposing BON-1 cells to 50 μM of Ru-bdcurc. The results demonstrated that the Ru-bdcurc/Brusatol combination increased BON-1 cell death (Fig. 3A, upper panel), compared with the 50 μM dose Ru-bdcurc alone. At the biochemical level, the Ru-bdcurc/Brusatol combination

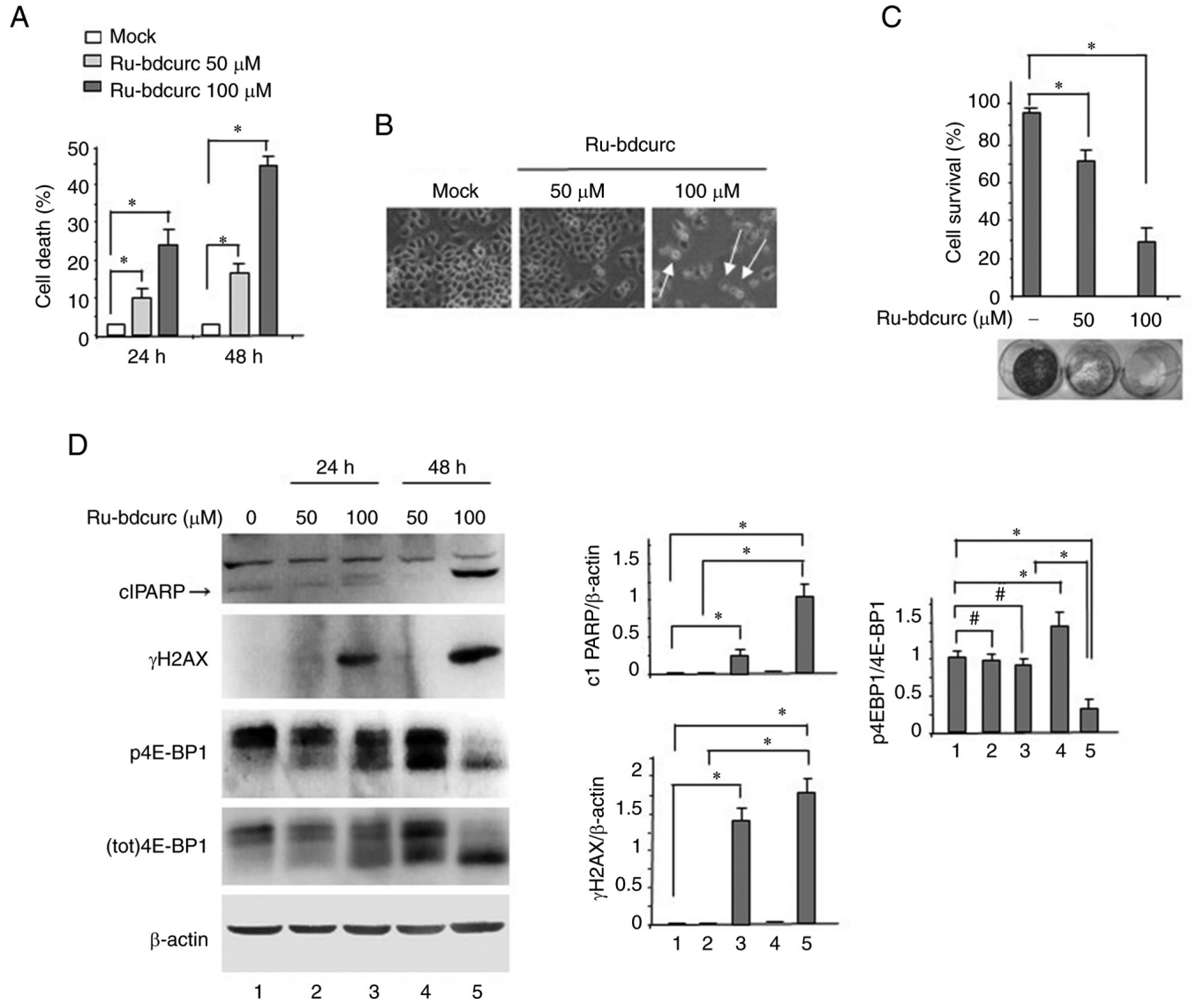

Figure 1. Ru-bdcurc induces dose- and time-dependent cell death in BON-1 cells. (A) BON-1 cells were left untreated or treated with different doses of Ru-bdcurc (50 and 100 μM) for 24 and 48 h before cell viability was measured by Trypan blue staining. Statistics was measured between treated (50 or 100 μM) and the untreated cells (Mock). (B) Live cell images were captured by light microscopy at x80 magnification to assess cell death (white arrows) of cells treated as in. (A) One representative image is shown. (C) Cell survival as measured by colony formation assay. Histograms represent the intensity of the cell staining quantified by ImageJ software. Below the histograms, a representative picture of BON-1 cells' death-resistant colonies stained with crystal violet is presented. Statistics was measured between treated (50 or 100 μM) and the untreated cells (-). (D) Western blot analysis of the indicated proteins levels in BON-1 cells treated as in. (A) β-actin were used to confirm equal protein loading, and one representative experiment is shown. The ratio of the protein levels vs. β-actin, following densitometric analysis, is reported. Statistics was measured between treated (50 or 100 μM) and the untreated cells (-) at 24 and 48 h. The histograms represent the mean ± SD. *P≤0.05 and $^{\#}$, not statistically significant. Ru-bdcurc, Ruthenium (Ru)(II)-Bisdemethoxycurcumin.

counteracted the Ru-bdcurc-induced upregulation of NRF2 as well as of its target p62 (Fig. 3A, lower panels); in addition, the Ru-bdcurc/Brusatol combination significantly increased the expression of γH2AX compared with the 50 μM dose of Ru-bdcurc alone (Fig. 3A, lower panels). Similarly, knocking down NRF2 by specific siRNA (Fig. 3B) increased the cell death induced by 50 μM dose of Ru-bdcurc compound (Fig. 3C, left panels). At the biochemical level, the NRF2 silencing reduced catalase and p62 expression, as well as the p53 levels that were induced in response to 50 μM dose of Ru-bdcurc (Fig. 3C, right panels), suggesting that an interplay between NRF2 and dysfunctional p53 exists in BON-1 cells. In addition, the Ru-bdcurc/Brusatol combination significantly increased the expression of γH2AX compared with the 50 μM dose of Ru-bdcurc alone (Fig. 3C, lower panels). Collectively, these results suggested that inhibiting the NRF2 pathway, induced by the lower dose of Ru-bdcurc, increased the cytotoxic effect of Ru-bdcurc compound.

Targeting p53 reduces NRF2 activation and increases the cytotoxic effect of 50 μM dose of Ru-bdcurc. Then, to evaluate the role of p53 in BON-1 cell response to the Ru-bdcurc compound and its interplay with NRF2, it was attempted to inhibit it by specific siRNA (38,39). The results demonstrated that knocking down p53 (Fig. 4A) reduced the Ru-bdcurc-induced upregulation of NRF2 and of its targets p62 and catalase (Fig. 4B). At the biological level, knocking down p53 increased the cell death induced by 50 μM dose of

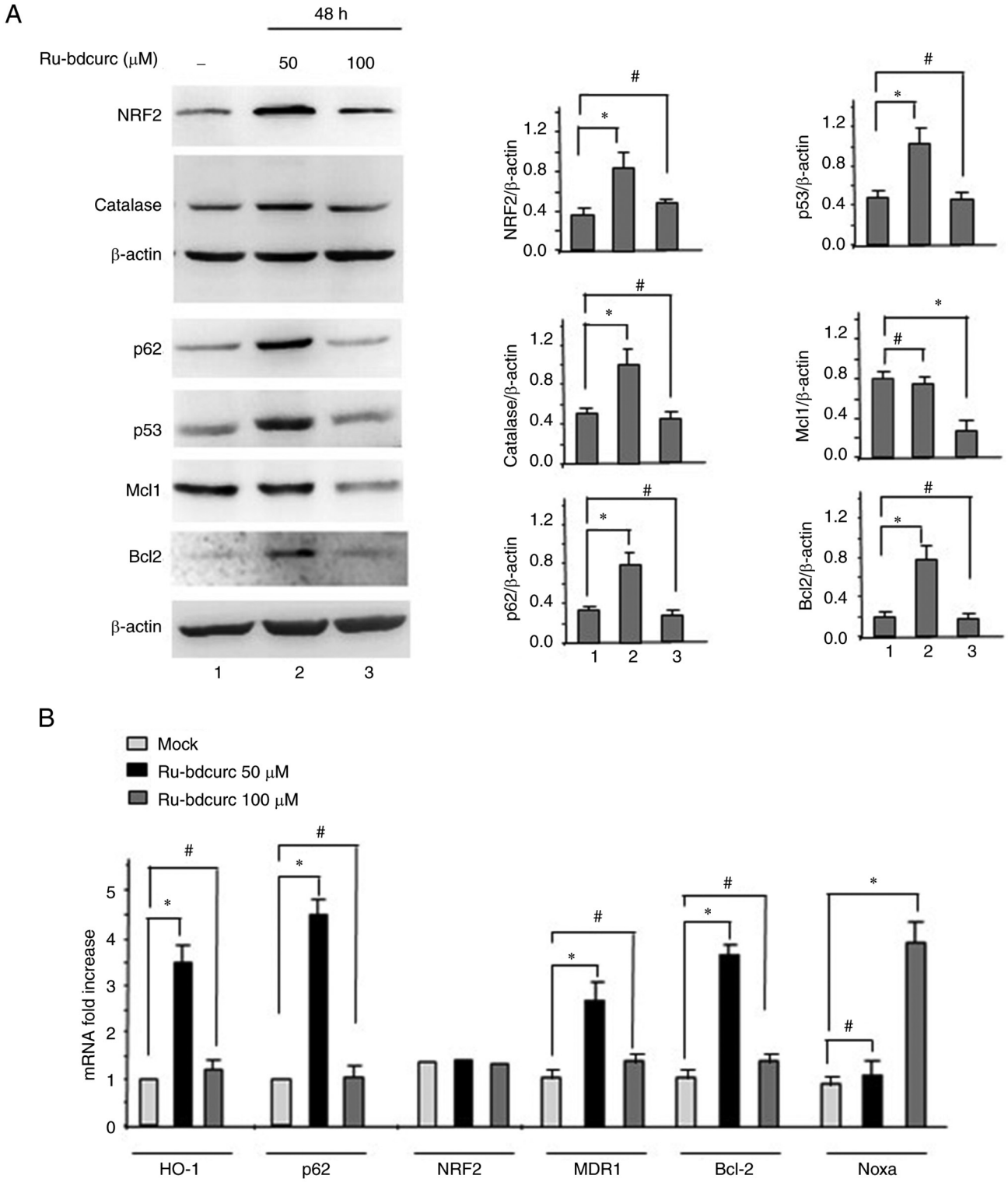

Figure 2. NRF2 activation in response to Ru-bdcurc. (A) BON-1 cells were treated with Ru-bdcurc (50 and 100 μM) for 48 h and the protein levels of NRF2, catalase, p62, p53, Mcl1 and Bcl2 proteins were evaluated by western blot analysis; β-actin was used as protein loading control and one representative experiment is shown. The ratio of the protein levels vs. β-actin, following densitometric analysis, is reported as histograms plus SD. Statistics was measured between treated (50 or 100 μM) and the untreated cells (-). (B) Total mRNA was extracted from cells treated as in (A) to evaluate HO-1, NRF2, p62, MDR1, Bcl-2 and Noxa gene expression by semiquantitative reverse transcription PCR of reverse transcribed cDNA. Histograms represent the mean ± SD of three independent experiments. Statistics was measured between treated (50 or 100 μM) and the untreated cells (Mock). *P≤0.05 and $^{\#}$, not statistically significant. NRF2, nuclear factor erythroid 2-related factor 2; Ru-bdcurc, Ruthenium (Ru)(II)-Bisdemethoxycurcumin.

Ru-bdcurc (Fig. 4C). Taken together, these results indicated that a dysfunctional endogenous p53 in BON-1 contributed to cellular resistance to Ru-bdcurc cytotoxicity, likely in an interplay with NRF2.

Discussion

In the present study, it was revealed that the novel Ru-bdcurc compound (16) was able to induce cell death in the pancreatic

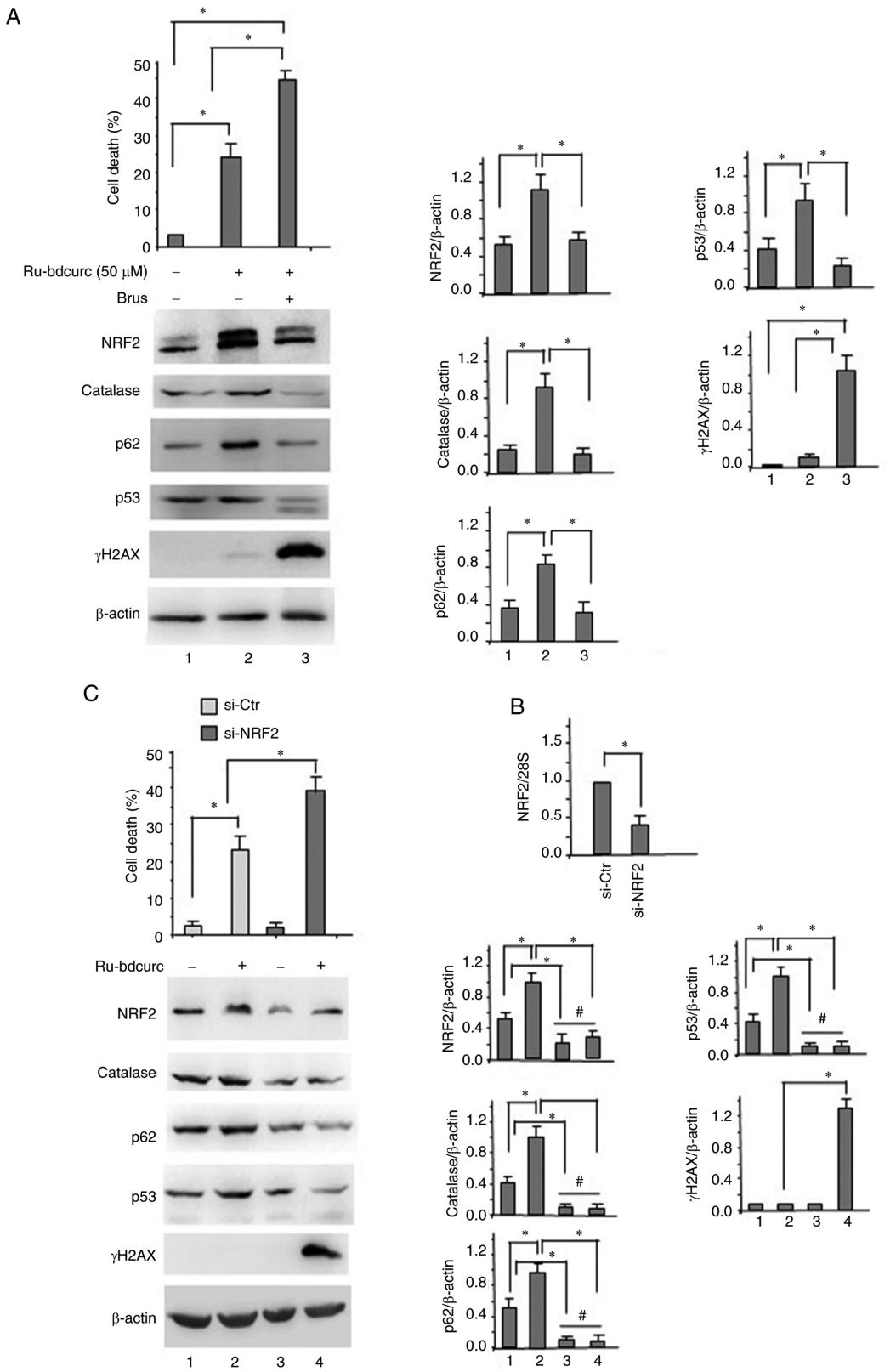

Figure 3. Pharmacologic or genetic inhibition of NRF2 improves the 50 μM Ru-bdcurc cytotoxic activity. (A) BON-1 cells were left untreated or pre-treated with 100 nM Brus for 4 h and then treated with 50 μM Ru-bdcurc for 48 h, before cell viability was measured by Trypan blue exclusion assay (upper panel). Protein levels were evaluated by western blot analysis (lower panel). β-actin was used as protein loading control and one representative experiment is shown. The ratio of the protein levels vs. β-actin, following densitometric analysis, is reported as histograms plus SD (right panels). Statistics was measured between treated (50 μM) and untreated cells (-) with or without Brus co-treatment. (B) BON-1 cells were transfected with siRNA control (si-ctr) or siNRF2 and, 24 h after transfection, NRF2 mRNA was evaluated by semiquantitative reverse transcription PCR. (C) BON-1 cells, transfected as in (B) for siRNA interference, were treated, 24 h after siRNA transfection, with Ru-bdcurc (50 μM) for 48 h before cell viability was measured by Trypan blue exclusion assay (upper panel). Protein levels were evaluated by western blot analysis (lower panel). β-actin was used as protein loading control and one representative experiment is shown. The ratio of the protein levels vs. β-actin, following densitometric analysis is reported as histograms plus SD (right panels). Statistics was measured between treated (50 μM) and untreated cells (-) and compared according to NRF2 interference. *P≤0.05 and #, not statistically significant. NRF2, nuclear factor erythroid 2-related factor 2; Ru-bdcurc, Ruthenium (Ru)(II)-Bisdemethoxycurcumin; Brus, brusatol; siRNA, small interfering RNA.

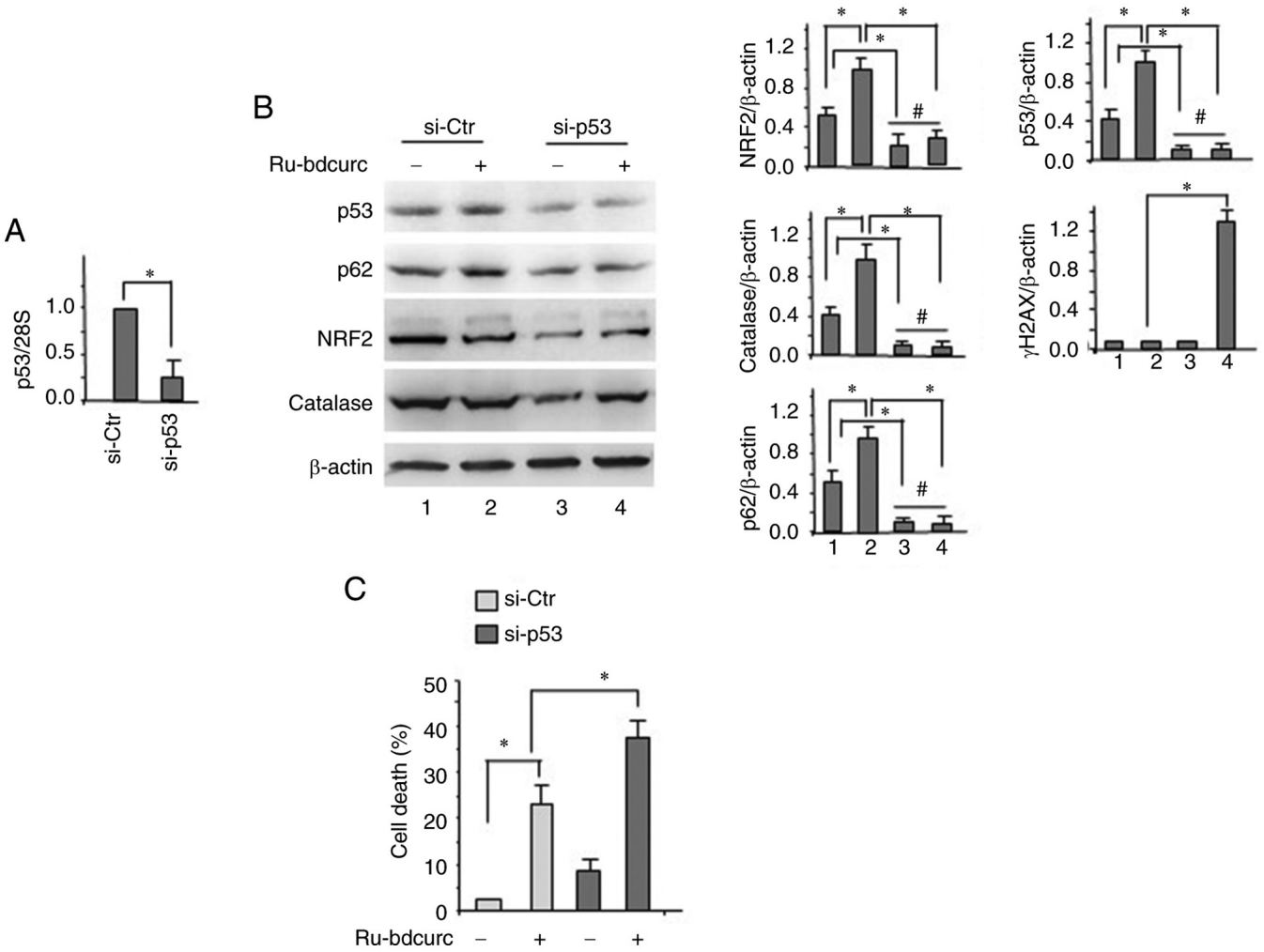

Figure 4. Dysfunctional-p53 cross-talks with NRF2 to reduce BON-1 chemosensitivity. (A) BON-1 cells were transfected with siRNA control (si-ctr) and sip53 and, 24 h after transfection, p53 mRNA was evaluated by semiquantitative reverse transcription PCR. (B) BON-1 cells, transfected as in (A) for siRNA interference were treated, 24 h after siRNA transfection, with Ru-bdcurc (50 μM) for 48 h. Protein levels were evaluate by western blot analysis. β-actin was used as protein loading control and one representative experiment is shown. The ratio of the proteins level vs. b-actin, following densitometric analysis, is reported as histograms plus SD (right panels). (C) Trypan blue exclusion assay was performed to asses viability of cells treated as in. (B) Statistics was measured between treated (50 μM) and untreated cells (-) and compared according to p53 interference. *P≤0.05 and #, not statistically significant. NRF2, nuclear factor erythroid 2-related factor 2; siRNA, small interfering RNA; Ru-bdcurc, Ruthenium (Ru)(II)-Bisdemethoxycurcumin.

NET cell line BON-1, in a dose-dependent way (Fig. 5A). Intriguingly, the higher dose of Ru-bdcurc (i.e., 100 μM) induced apoptotic cell death while the lower dose (i.e, 50 μM) induced chemoresistant pathways that reduced the cytotoxic activity of the compound. The 100 μM dose of Ru-bdcurc treatment increased the clPARP/PARP ratio, compared with 50 μM dose, and correlated with the appearance of the phosphorylated form of H2AX (γH2AX), a marker of DNA damage and apoptosis (48). Moreover, 100 μM dose of Ru-bdcurc induced the expression of Noxa, a pro-apoptotic gene induced by p53 family members (56), that has been reported to inhibit the antiapoptotic Mcl1 protein (57), in agreement with the reduction of Mcl1 protein levels in Fig. 2A. On the other hand, 50 μM dose of Ru-bdcurc induced the phosphorylation of 4EBP1 (p4E-BP1), a mTOR target whose activation can sustain cancer cell survival and predict poor prognosis (49,50). In agreement, mTOR pathway has been found to be dysregulated in GEP-NET and involved in tumor development (51). The 50 μM dose of Ru-bdcurc activated the NRF2 pathway with upregulation of its targets p62 and catalase, increased the antiapoptotic Bcl-2 protein levels and the endogenous dysfunctional p53 protein levels. The increased p62 gene expression was in accordance with the finding that p62 is a NRF2 transcriptional target (23-25). The reason why only the lower dose of Ru-bdcurc induced NRF2 activity remains not completely resolved at the molecular level. From the literature it is known that curcumin can induce NRF2 through activation of p62 by phosphorylation (58), therefore it can be hypothesized that only the lower dose of Ru-bdcurc might induce the kinases involved in p62 posttranslational modifications in order to be activated. Interestingly, it has been revealed that p62 activates pro-survival pathways including mTOR (52), in agreement with the aforementioned results in Fig. 1 and with the cross-talk among oncogenic pathways such as p62/mTOR/NRF2 to increase tumor development and resistance to therapies (30). Moreover, only the 50 μM dose of Ru-bdcurc treatment, compared with 100 μM dose, increased the endogenous p53 protein level, in agreement with the paradigm that the interplay between NRF2 and mutp53

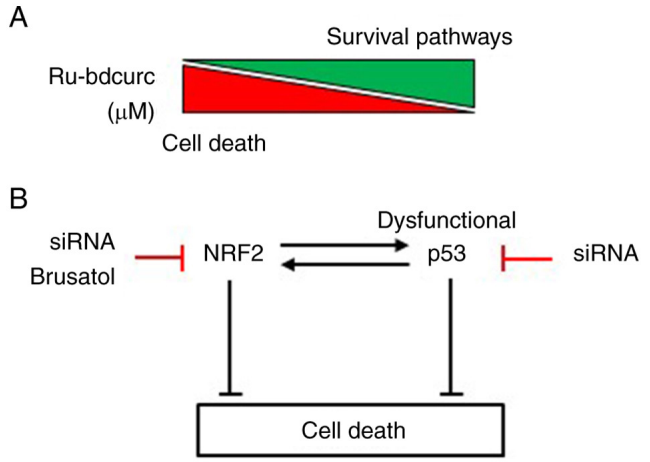

Figure 5. Graphical representation of cell response to Ru-bdcurc treatment. (A) The graph illustrates that higher doses of Ru-bdcurd induced cell death while lower doses induced cell survival pathways. (B) Activation of the NRF2 pathway could stabilize also mutant/dysfunctional p53 and both pathways contributed to inhibition of drug-induced cell death. Silencing of p53 or NRF2 (red symbols) could overcome their chemoresistant mechanisms and improve the cell death. Ru-bdcurc, Ruthenium (Ru)(II)-Bisdemethoxycurcumin; NRF2, nuclear factor erythroid 2-related factor 2; siRNA, small interfering RNA.

stabilizes each other proteins to sustain their oncogenic activities (41,54). The endogenous p53 has been reported to be dysfunctional in BON-1 cells and to inhibit apoptosis (28). Thus, in this study the wild-type p53 target genes were not detected after cell treatment with 50 μM dose of Ru-bdcurc (data not shown), suggesting lack of p53 wild-type activity. On the other hand, 50 μM dose of Ru-bdcurc, compared with 100 μM, induced the expression of MDR1, a target of some mutant p53 proteins (55), as well as of the antiapoptotic gene Bcl-2, which associated with a potential oncogenic activity of the endogenous dysfunctional p53 in BON-1 cells. Interestingly, 100 μM dose of Ru-bdcurc induced cell death that correlated with the expression of Noxa a pro-apoptotic gene induced by p53 but also by p53 family members such as p73 (56). The fact that p53 protein expression did not increase after 100 μM dose of Ru-bdcurc but rather decreased (Fig. 4B) can suggest that mutant/dysfunctional p53 in BON-1 cells was downregulated in agreement with NRF2 downregulation but that this downregulation did not reactivate a potential endogenous wild-type p53 gene, suggesting that p53 family members, rather than wild-type p53, were inducing Noxa mRNA expression. However, further experiments are necessary to validate the endogenous p53 status in BON-1 cells and its or not reactivation after curcumin treatment. Mutations in p53 gene are reported in ~90-95% of GEP-NEC and in 3% of GEP-NET (59); however, the endogenous mutant p53 activity in BON-1 needs to be explored in future studies. Inhibiting the NRF2 pathway by genetic or pharmacologic means increased the cytotoxic effect of the lower dose of the Ru-bdcurc compound. Similarly, silencing of the endogenous dysfunctional p53 counteracted the NRF2 activation in response to the lower dose of Ru-bdcurc and increased the cytotoxic effect of the compound, strongly supporting the oncogenic interplay between NRF2 and p53 in this setting (Fig. 5B). GEP-NEN are extremely heterogeneous tumors and identifying potential biomarkers for therapeutic purpose is difficult. In the present study, one potential pathway of chemoresistance to be validated in tumor samples, was suggested. However, the limitation of the present study is the use of only one cell line, despite the cell lines available for this type of tumors are only two (27-29). It was also attempted to perform the experiments in the QGP-1 cell line but it was not possible not obtain the same results as in BON-1. QGP-1 cell line carries a wtp53 but does not present NRF2 induction after treatment, as observed in BON-1 cells, at least in the present experiments. Given that these tumors are genetically different it becomes very difficult to generalize the results between the two cell lines. Therefore, additional studies are necessary to clearly establish a role for NRF2 and the interconnected oncogenic molecular pathways in tumors *in vivo*.

The results of the present study can be discussed in view of the potential effects of curcumin treatment in patients; In particular, the low versus the high dose of curcumin that can be achieved *in vivo* in patients. Thus, in clinical trials high dose of curcumin ends often in low plasma level of curcumin (60,61) likely due to curcumin low solubility and bioavailability and low curcumin doses have been shown to act as an antioxidant agent and do not induce cell death, thus contributing to acquired chemoresistance (62). For this reason, the use of more soluble and assimilable compounds such as the organometallic ruthenium ones (12-14), used in the present study, could be taken in consideration in clinical practice. On the other side, combination therapies with curcumin compounds and more classical chemotherapeutic agents should include also molecules that target the NRF2 pathway to inhibit not only NRF2 but also the interconnected oncogenic pathways that often interact with it to increase tumor resistance to therapies. In agreement, previous studies have reported that targeting NRF2 is a promising strategy for the treatment of several aggressive cancers where the activation of the NRF2 pathway protects cancer cells from the cytotoxic effects of the chemotherapeutic drugs (63-66). In conclusion, the results of the present study demonstrated for the first time, to the best of the authors' knowledge, that NRF2 may play a role in chemoresistance of the pancreatic neuroendocrine BON-1 cancer cells and suggested to evaluate the NRF2-dependent pathway as a potential biomarker in GEP-NENs tissues. If this hypothesis is confirmed in GEP-NENs, NRF2 pathway could become a novel biomarker to be taken in consideration to tailor more effective cytotoxic therapies against this type of rare tumor that remains an orphan-drug cancer.

Acknowledgements

The authors would like to thank Dr Elisa Melucci (Regina Elena National Cancer Institute; Rome, Italy) for technical support.

Funding

The present study was supported by the Italian Association for Cancer Research (AIRC) (grant nos. Id16742 and Id23040) and by the University of Camerino (Fondo di Ateneo per la Ricerca-University Research; grant no: 2018).

Availability of data and materials

The datasets used and/or analyzed during the current study are available from the corresponding author on reasonable request.

Authors' contributions

GDO, AG, MC, SS, MA, RP and FM conceptualized the study. RP and FM developed methodology. AG, LM, GP, IV and GDO curated data. GDO wrote the original draft. GDO, AG. MC, SS and FM wrote, reviewed and edited the manuscript. GDO, SS and FM supervised the study. GDO, MC and FM acquired funding. AG and LM confirm the authenticity of all the raw data. All authors have read and approved the final version of the manuscript.

Ethics approval and consent to participate

Not applicable.

Patient consent for publication

Not applicable.

Competing interests

The authors declare that they have no competing interests.

References

1. Rindi G, Mete O, Uccella S, Basturk O, La Rosa S, Brosens LAA, Ezzat S, de Herder WW, Klimstra DS, Papotti M and Asa SL: Overview of the 2022 WHO Classification of Neuroendocrine Neoplasms. Endocr Pathol 33: 115-154, 2022.
2. Cives M and Strosberg JR: Gastroenteropancreatic neuroendocrine tumors. CA Cancer J Clin 68: 471-487, 2018.
3. Huguet I, Grossman AB and O'Toole D: Changes in the epidemiology of neuroendocrine tumours. Neuroendocrinology 104: 105-111, 2017.
4. Norton JA: Surgery for primary pancreatic neuroendocrine tumors. J Gastrointest Surg 10: 327-331, 2006.
5. Akirov A, Larouche V, Alshehri S, Asa SA and Ezzat S: Treatment options for pancreatic neuroendocrine tumors. Cancers 11: 828, 2019.
6. Das S, Al-Toubah T and Strosberg J: Chemotherapy in neuroendocrine tumors. Cancers 13: 4872, 2021.
7. Dai M, Mullins CS, Lu L, Alsfasser G and Linnebacher M: Recent advances in diagnosis and treatment of gastroenteropancreatic neuroendocrine neoplasms. World J Gastrointest Surg 14: 383-396, 2022.
8. Haque A, Brazeau D and Amin AR: Perspectives on natural compounds in chemoprevention and treatment of cancer: An update with new promising compounds. Eur J Cancer 149: 165-183, 2021.
9. Patel SS, Acharya A, Ray RS, Agrawal R, Raghuwanshi R and Jain P: Cellular and molecular mechanisms of curcumin in prevention and treatment of disease. Crit Rev Food Sci Nutr 60: 887-939, 2020.
10. Zoi V, Galani V, Lianos GD, Voulgaris S, Kyritsis AP and Alexiou GA: The role of curcumin in cancer treatment. Biomedicines 9: 1086, 2021.
11. Stohs SS, Chen O, Ray SD, Ji J, Bucci LR and Preuss HG: Highly bioavailable forms of curcumin and promising avenues for Curcumin-Based research and application. Molecules 25: 1397, 2020.
12. Wanninger S, Lorenz V, Subhan A and Edelmann FT: Metal complexes of curcumin-synthetic strategies, structures and medicinal applications. Chem Soc Rev 44: 4986-5002, 2015.
13. Pagliaricci N, Pettinari R, Marchetti F, Pettinari C, Cappellacci L, Tombesi A, Cuccioloni M, Hadiji M and Dyson PJ: Potent and selective anticancer activity of half-sandwich ruthenium and osmium complexes with modified curcuminoid ligands. Dalton Trans 51: 13311-13321, 2022.
14. Gobbo A, Pereira SAP, Biancalana L, Zacchini S, Saraiva MLMFS, Dyson PJ and Marchetti F: Anticancer ruthenium(II) tris(pyrazolyl)methane complexes with bioactive co-ligands. Dalton Trans 51: 17050-17063, 2022.
15. Bonfili L, Pettinari R, Cuccioloni M, Cecarini V, Mozzicafreddo M, Angeletti M, Lupidi G, Marchetti F, Pettinari C and Eleuteri AM: Arene-RuII complexes of curcumin exert antitumor activity via proteasome inhibition and apoptosis induction. Chem Med Chem 7: 2010-2020, 2012.
16. Pettinari R, Marchetti F, Condello F, Pettinari C, Lupidi G, Scopelliti R, Mukhopadhyay S, Riedel T and Dyson PJ: Ruthenium(II)-Arene RAPTA type complexes containing curcumin and bisdemethoxycurcumin display potent and selective anticancer activity. Organometallics 33: 3709-3715, 2014.
17. Caruso F, Pettinari R, Rossi M, Monti E, Gariboldi MB, Marchetti F, Pettinari C, Caruso A, Ramani MV and Subbaraju GVJ: The in vitro antitumor activity of arene-ruthenium(II) curcuminoid complexes improves when decreasing curcumin polarity. J Inorg. Biochem 162: 44-51, 2016.
18. Garufi A, Baldari S, Pettinari R, Gilardini Montani MS, D'Orazi V, Pistritto G, Crispini A, Giorno E, Toietta G, Marchetti F, *et al*: A ruthenium(II)-curcumin compound modulates NRF2 expression balancing the cancer cell death/survival outcome according to p53 status. J Exp Clin Cancer Res 39: 122, 2020.
19. Garufi A, Pettinari R, Marchetti F, Cirone M and D'Orazi G: NRF2 and Bip interconnection mediates resistance to the organometallic ruthenium-cymene bisdemethoxycurcumin complex cytotoxicity in colon cancer cells. Biomedicines 11: 593, 2023.
20. D'Orazi G and Cirone M: Interconnected adaptive responses: A way out for cancer cells to avoid cellular demise. Cancers 14: 2780, 2022.
21. Garufi A, Pistritto G, D'Orazi V, Cirone M and D'Orazi G: The impact of NRF2 inhibition on drug-induced colon cancer cell death and p53 activity: A pilot study. Biomolecules 2: 461, 2022.
22. Rojo de la Vega M, Chapman E and Zhang DD: NRF2 and the hallmarks of cancer. Cancer Cell 34: 21-43, 2018
23. Jain A, Lamark T, Sjottem E, Bowitz Larsen K, Awuh JA, Overvatn A, McMahon M, Hayes JD and Johansen T: p62/SQSTM1 is a target gene for transcription factor NRF2 and creates a positive feedback loop by inducing antioxidant response element-driven gene transcription. J Biol Chem 285: 22576-22591, 2010.
24. Komatsu M, Kurokawa H, Waguri S, Taguchi K, Kobayashi A, Ichmura Y, Sou YS, Ueno I, Sakamoto A, Tong KI, *et al*: The selective autophagy substrate p62 activates the stress response transcription factor Nrf2 through inactivation of Keap1. Nat Cell Biol 12: 213-23, 2010.
25. Jiang T, Harder B, Rojo de la Vega M, Wong PK, Chapman E and Zhang DD: p62 links autophagy and Nrf2 signaling. Free Rad Biol Med 88: 199-204, 2015.
26. Lister A, Nedjadi T, Kitteringham NR, Campbell F, Costello E, Lloyd B, Copple IM, Williams S, Owen A, Neoptolemos JP, *et al*: Nrf2 is overexpressed in pancreatic cancer: Implications for cell proliferation and therapy. Mol Cancer 10: 37, 2011.
27. Evers BM, Ishizuka J, Townsend CM Jr and Thompson JC: The human carcinoid cell line, BON. A model system for the study of carcinoid tumors. Ann N Y Acad Sci 733: 393-406, 1994.
28. Vandamme T, Peeters M, Dogan F, Pauwels P, Van Assche E, Beyens M, Mortier G, Vandeweyer G, de Herder W, Van Camp G, *et al*: Whole-exome characterization of pancreatic neuroendocrine tumor cell lines BON-1 and QGP-1. J Mol Endocrinol 54: 137-47, 2015.
29. Luley KB, Biedermann SB, Kunstner A, Busch H, Franzenburg S, Schrader J, Grabowsi P, Wellner U, Keck T, Brabant G, *et al*: A comprehensive molecular characterization of the pancreatic neuroendocrine tumor cell lines BON-1 and QGP-1. Cancers (Basel) 12: 691, 2020.
30. Cirone M and D'Orazi G: NRF2 in cancer: Cross-talk with oncogenic pathways and involvement in gammaherpesviruses-driven carcinogenesis. Int J Mol Sci 24: 595, 2022.
31. Vousden HK and Prives C: Blinded by the light: The growing complexity of p53. Cell 137: 413-31, 2009
32. Muller PA and Vousden KH: Mutant p53 in cancer: New functions and therapeutic opportunities. Cancer Cell 25: 304-317, 2014.

33. Voutsadakis IA: Mutations of p53 associated with pancreatic cancer and therapeutic implications. Ann Hepatobiliary Pancreat Surg 25: 315-327, 2021.
34. Vijayvergia N, Boland PM, Handorf E, Gustafson KS, Gong Y, Cooper HS, Sheriff F, Astsaturov I, Cohen SJ and Engstrom PF: Molecular profiling of neuroendocrine malignancies to identify prognostic and therapeutic markers: A Fox Chase Cancer Center Pilot Study. Br J Cancer 115: 564-570, 2016.
35. Ren D, Villeneuve NF, Jiang T, Wu T, Lau A and Toppin HA: Brusatol enhances the efficacy of chemotherapy by inhibiting the Nrf2-mediated defense mechanism. Proc Natl Acad Sci USA 108: 1433-1438, 2011.
36. Olayanju A, Copple IM, Bryan HK, Edge GT, Sison RL, Wong MW, Lai ZQ, Lin ZX, Dunn K, Sanderson CM, *et al*: Brusatol provokes a rapid and transient inhibition of Nrf2 signaling and sensitizes mammalian cells to chemical toxicity implications for therapeutic targeting of Nrf2. Free Rad Biol Med 78: 202-12, 2015.
37. Garufi A, Traversi G, Gilardini Montani MS, D'Orazi V, Pistritto G, Cirone M and D'Orazi G: Reduced chemotherapeutic sensitivity in high glucose condition: implication of antioxidant response. Oncotarget 10: 4691-4702, 2019.
38. Cecchinelli B, Lavra L, Rinaldo C, Iacovelli S, Gurtner A, Gasbarri A, Ulivieri A, Del Prete F, Trovato M, Piaggio G, *et al*: Repression of the antiapoptotic molecule galectin-3 by homeodomain-interacting protein kinase 2-activated p53 is required for p53-induced apoptosis. Mol Cell Biol 26: 4746-4757, 2006.
39. Brummelkamp TR, Bernards R and Agami R: A system stable expression of short interfering RNAs in mammalian cells. Science 296: 550-553, 2020.
40. Garufi A, Giorno E, Gilardini Montani MS, Pistritto G, Crispini A, Cirone M and D'Orazi G: P62/SQSTM1/Keap1/NRF2 axis reduces cancer cells death-sensitivity in response to Zn(II)-curcumin complex. Biomolecules 11: 348, 2021.
41. Lisek K, Campaner E, Ciani Y, Walerych D and Del Sal G: Mutant p53 tunes the NRF2-dependent antioxidant response to support survival of cancer cells. Oncotarget 9: 20508-20523, 2018
42. Gong C, Yao H, Liu Q, Chen J, Shi J, Su F and Song E: Markers of tumor-initiating cells predict chemoresistance in breast cancer. PLoS One 5: e15630, 2010.
43. Garufi A, Pistritto G, Cirone M and D'Orazi G: Reactivation of mutant p53 by capsaicin, the major constituent of peppers. J Exp Clin Cancer Res 35: 136, 2016.
44. Gilles C, Polette M, Mestdagt M, Nawrocki-Raby B, Ruggeri P, Birembaut P and Foidart JM: Transactivation of vimentin by beta-catenin in human breast cancer cells. Cancer Res 15: 2658-2664, 2003.
45. Nodale C, Sheffer M, Jacob-Hirsch J, Folgiero V, Falcioni R, Aiello A, Garufi A, Rechavi G, Givol D and D'Orazi G: HIPK2 downregulates vimentin and inhibits breast cancer cell invasion. Cancer Biol Ther 13: 198-205, 2012.
46. Garufi A, Trisciuoglio D, Porru M, Leonetti C, Stoppacciaro A, D'Orazi V, AVantaggiati ML, Crispini A, Pucci D and D'Orazi G: A fluorescent-based Zn(II)-complex reactivates mutant (R175H and R272H) p53 in cancer cells. J Exp Clin Cancer Res 32: 72, 2013.
47. Garufi A, Pucci D, D'Orazi V, Cirone M, Bossi G, Avantaggiati ML and D'Orazi G: Degradation of mutant p53H175 protein by Zn(II) through autophagy. Cell Death Dis 5: e1271, 2014.
48. Bonner WM, Redon CE, Dickey JS, Nakamura AJ, Sedelnikova OA, Solier S and Pommier Y: Gamma H2AX and cancer. Nat Rev Cancer 8: 957-967, 2008.
49. Miao Y, Chen L, Shi C, Fan R, Chen P, Liu H, Xia A and Qin H. Increased phosphorylation of 4E-binding protein 1 predicts poor prognosis for patients with colorectal cancer. Mol Med Rep 15: 3099-3104, 2017.
50. Gonnella R, Zarrella R, Santarelli R, Germano CA, Gilardini Montani MS and Cirone M: Mechanisms of sensitivity and resistance of primary effusion lymphoma to Dimethyl Fumarate (DMF). Int J Mol Sci 23: 6773, 2022.
51. Zanini S, Renzi S, Giovinazzo F and Bermano G: mTOR pathway in gastroenteropancreatic neuroendocrine tumor (GEP-NETs). Front Endocrinol 11: 562505, 2020.
52. Moscat J, Karin M and Diaz-Meco MT: p62 in cancer: Signaling adaptor beyond autophagy. Cell 167: 606-609, 2016.
53. Widden H and Placzek WJ: The multiple mechanisms of Mcl1 in the regulation of cell fate. Commun Biol 4: 1029, 2021.
54. Gilardini Montani MS, Cecere N, Granato M, Romeo MA, Falcinelli L, Ciciarelli U, D'Orazi G, Faggioni A and Cirone M: Mutant p53, stabilized by its interplay with HSP90, activates a positive feed-back loop between NRF2 and p62 that induces chemo-resistance to Apigenin in pancreatic cancer cells. Cancers 11: 703, 2019.
55. Sampath J, Sun D, Kidd VJ, Grenet J, Gandhi A, Shapiro LH, Wang Q, Zambetti GP and Schuetz JD: Mutant p53 cooperates with ETS and selectively up-regulates human MDR1 not MRP1. J Biol Chem 276: 39359-39367, 2001
56. Martin AG, Trama J, Crighton D, Ryan KM and Fearnhead HO: Activation of p53 and induction of Noxa by DNA damage requires NG-kappa B. Aging (Albany NY) 1: 335-349, 2009.
57. Chiou JT, Huang NC, Hiang CH, Wang LJ, Lee YC, Shi YJ and Chang LS: NOXA-mediated degradation of MCL1 and BCL2L1 causes apoptosis of daunorubicin-treated human acute myeloid leukemia cells. J Cell Physiol 236: 7356-7375, 2021.
58. Park JY, Sohn HY, Koh YH and Jo C: Curcumin activates Nrf2 through PKCd-mediated p62 phosphorylation at Ser351. Sci Rep 11: 8430, 2021.
59. Kawasaki K, Fujii M and Sato T: Gastroenteroepatic neuroendocrine neoplasms: Genes, therapies and models. Dis Model Mech 11: dmm029595, 2018.
60. Cao J, Jia L, Zhou HM, Liu Y and Zhong LF: Mitochondrial and nuclear DNA damage induced by curcumin in human hepatoma G2 cells. Toxicol 91: 476-483, 2006.
61. Kunati SR, Yang SM, William BM and Xu Y: An LC-MS/MS method for simultaneous determination of curcumin, curcumin glucuronide and curcumin sulfate in a phase II clinical trial. J Pharm Biomed Anal 156: 189-198, 2018.
62. Giordano A and Tommonaro G: Curcumin and Cancer. Nutrients 11: 2376, 2019.
63. Arena A, Romeo MA, Benedetti R, Gilardini Montani MS, Santarelli R, Gonnella R, D'Orazi G and Cirone M: NRF2 and STAT3: Friends or foes in carcinogenesis? Discov Oncol 14: 37, 2023.
64. Sajadimajd S and Khazaei M: Oxidative stress and cancer: The role of Nrf2. Curr Cancer Drug Targtes 18: 538-557, 2018.
65. No JH, Kim YB and Song YS: Targeting Nrf2 signaling to combat chemoresistance. J Cancer Prev 19: 111-117, 2014.
66. Torrente L and DeNicola GM: Targeting NRF2 and its downstream processes: Opportunities and challenges. Annu Rev Pharmacol Toxicol 62: 279-300, 2022.